Searches for diboson resonances at the LHC

Project report

PHYS11063 - Current Topics in Particle Physics

s2092468

Contents

1 Introduction

One of the main physics objectives of the LHC is to search broad areas of the phase space for final decay states that could be a sign of Beyond the Standard Model (BSM) physics. This push is motivated by the Standard Model's unsatisfactory explanations of fundamental physical phenomena such as the matter-antimatter imbalance, the excess amounts of charge-parity (CP) violation, the fine-tuning in the Higgs mass, the identity of dark matter, and the incompatibility with General Relativity.

In the search for solutions to these unresolved issues, numerous theories that extend the Standard Model have been proposed. These theories frequently introduce new particles or interactions operating at the TeV scale which, according to some models, we can detect as diboson decays[1]. This common signature is what makes these resonances particularly promising for probing BSM physics at the LHC.

2 The models

There are a large number of models first introduced to resolve specific issues within particle physics that were then found to predict diboson decays. On top of these, after some initially promising results at the end of run 1 at the LHC (see section 4.1), multiple papers were published presenting new possible explanations for the observed excesses[2]. Adding these two contributions together results in a wide range of models, primarily categorized as extended gauge models, models with warped extra dimensions, technicolor, or composite Higgs models.

In this section, we will first take a closer look at Technicolour as one of the first models that predicted diboson resonances and we will then explore the three benchmark models most often chosen by the CMS and ATLAS experiments.

2.1 Technicolour

Technicolour was first introduced to offer an alternative explanation to the spontaneous breaking of electro-weak symmetry. It proposes a new gauge interaction that couples to technifermions and can dynamically give the W and Z bosons their masses. This theory therefore does not consider the Higgs boson an elementary particle, eliminating the need for the fine-tuning required to explain its mass in the SM[3]. The claimed "naturalness" of this theory started to fall apart as more precise electro-weak measurements were performed posing limits on the effects of flavor-changing neutral currents and the discovery of the Higgs boson forced variants of Technicolour to fine-tune parameters to match predictions to the

experimental results. By the end of Run 1 at the LHC, one of the most viable remaining theories in the Technicolour family was Walking Technicolour, where the coupling constant of the new force does not run as quickly with energy as the QCD one does[4]. The one-family model of Walking Technicolour which proposes a single generation of 8 technifermions can account for the 125 GeV Higgs boson[5] and also predicts massive vector bosons called technirhos. More specifically, the ρ_π^3 isopsin-triplet of technirhos predicts couplings with SM W and Z bosons such that the decays $\rho_\pi^\pm \to WZ$ would be visible at the LHC[6].

2.2 Selecting three benchmark models

While Walking Technicolour and other specific models can account for diboson resonances, their particularity, the untestability of their other predictions, and the fine-tuning required to account for other SM observations make them bad candidates for benchmark models to be used for ATLAS and CMS diboson resonance searches. It is preferred that the models selected for this purpose be more general and parameterized so that conclusions drawn from them can be more easily reinterpreted in the future if new discoveries in the field are made.

Over the course of Run 1 and even more in Run 2, three models have emerged as the go-to benchmarks for diboson searches at the LHC. These are typically categorized based on the spin of the resonance they predict.

2.2.1 Spin 0

The spin 0 resonance is a new heavy scalar singlet S decaying into longitudinally polarized bosons. This can represent BSM particles like a new heavy Higgs like the one introduced by the Two Higgs Doublet Model[7] to account for missing CP violation in the SM, or the neutral scalar radion added in some Randall-Sundrum models to stabilise the radius of the warped extra dimension[8]. This model is parameterized by an energy scale Λ and by the coupling of S to the SM Higgs and gluons c_H and c_3 respectively. These can be adjusted to obtain varying decay widths to W and Z bosons[9], but the branching ratio to fermions is always chosen to be very small, if not zero. For this reason, the main production process for the scalar singlet is gluon gluon fusion, shown in the first Feynman diagram in figure 1. The decays predicted are $S \to WW$ and $S \to ZZ$.

2.2.2 Spin 1

The benchmark model for spin 1 resonances is the simplified HVT (Heavy Vector Triplet) parametrization that describes three new heavy bosons (two charged W' and one neutral Z'), degenerate in mass[9]. It parametrizes the couplings of the vector bosons to SM particles in

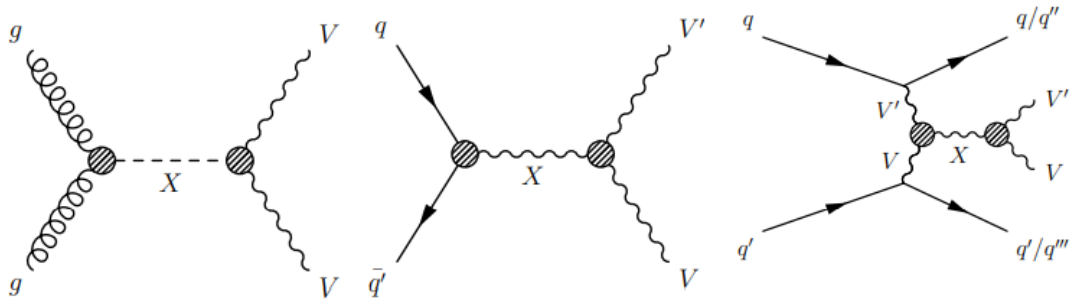

Figure 1: From left to right: Feynman diagrams of gluon-gluon fusion, Drell-Yan and vector-boson fusion production processes of a diboson resonance. Here V represents either W or Z bosons and X represents the unknown diboson resonance[10].

a generic way, allowing it to represent a wide range of models introduced to alleviate the hierarchy problem but also to derive model-independent phenomenology[11]. The coupling to fermions and the Higgs boson are described by $g^2 c_F / g_V$ and $g_V c_H$ respectively, where g is the electroweak gauge coupling, c_F and c_H are factors that scale the coupling to fermions and the Higgs, and g_V is the coupling to SM W/Z bosons.

Within this parameterization, two benchmarks are typically used. The first one, called Model A, with $g_V = 1$, represents weakly coupled models such as the sequential standard model and has couplings to SM W and Z bosons comparable to the one to fermions. The second one, Model B, sets $g_V = 3$ and represents strongly coupled models like Composite Higgs models where couplings to bosons are stronger compared to fermions. The main production process for the heavy vector bosons is via Drell-Yan interactions, but vector-boson fusion is also a significant process, especially when coupling to fermions is highly suppressed (see the second and third diagrams in figure 1). In both models, the decays predicted are $W' \to WZ$ and $Z' \to WW$.

2.2.3 Spin 2

The spin 2 resonance is most often modeled as G_{KK}, the first Kaluza-Klein excitation mode of gravitons predicted Randall-Sundrum (RS) models with an extra dimension with curvature κ, introduced to explain the weakness of gravity. More specifically, the RS model we are interested in is the bulk RS model where SM fields propagate in bulk as well as the 4D brane, as the original RS model has already been highly tested and constrained because its dominant decay modes are to fermions and photons[12]. Because of the reduced coupling to fermions in bulk models, the main production processes are gluon-gluon and vector-boson fusion, shown in the first and third diagrams in figure 1. The diboson decay modes predicted

are $G_{KK} \to WW$ and $G_{KK} \to ZZ$.

3 Experimental process

Now that we have discussed the models that give rise to diboson resonances, we will look at some aspects of the experimental process and what considerations we need to keep in mind that are specific to searches for these resonances.

3.1 V-tagging

One of the first steps of the experimental process is to identify and reconstruct the particles involved in the decays. In the decays of heavy particles like the ones we are searching for, the decay products will be highly boosted and in the case of hadronic decays, the resulting showers will involve collimated jets that tend to overlap with the other shower originating in the decay[12]. Treating this is crucial to V-tagging, the process of identifying the boson that decayed into the jets we see.

Because of the prominence of pile-up in these searches, the anti-k_t or Cambridge-Aachen sequential recombination algorithms used to reconstruct jets are usually run with two different radius parameters, producing the so-called large and small R jets. Large R jets incorporate the overlapping jets from a pair of boosted decaying particles and are post-processed to remove pileup effects and separate out the two particles' decay products.

An example of a very effective algorithm for this purpose is the PUPPI (Pile-Up Per Particle Identification) algorithm used at CMS[13]. It combines tracking information with event pile-up properties to reweight the four momenta of both charged and neutral particles based on their probability of originating from pile-up events and it discards charged particles not originating from the primary vertex[14]. In figure 2 we can see some run-time snapshots of the algorithm. The original uncontaminated jets (top left) are superposed with the pile-up effects in gray (top right). After the first part of the algorithm (bottom left) there is a reduction in the central density as charged particles not originating from the primary vertex have been removed. All the original jets are reconstructed at the end of the algorithm (bottom right).

3.2 Production residuals

The final states for resonances produced through vector-boson fusion differ from the other two production processes as they feature two additional jets. These can be tagged as VBF jets due to their large invariant mass and large angular separation in pseudorapidity[10].

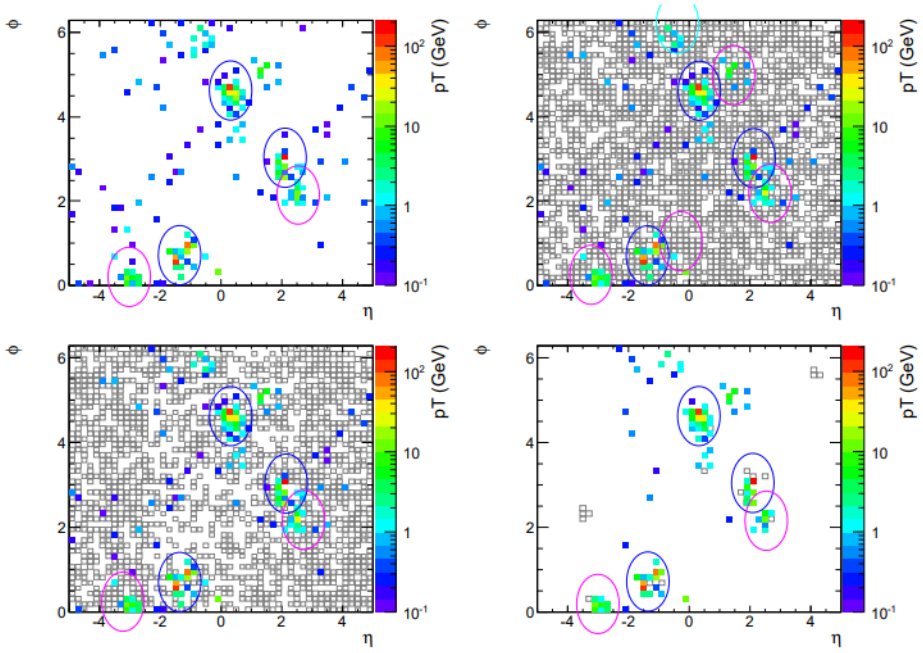

Figure 2: Progression of PUPPI in action. See text for more details.[13]

These characteristics can be used by recurrent neural networks to classify the VBF topology. Due to the effects these jets have on the rest of the process analyses are typically conducted separately for VBF-produced resonances, even within the same benchmark model.

3.3 Decay channels and backgrounds

Considering all the possible decay modes for W and Z bosons, there are numerous combinations of final states that need to be reconstructed. These are classified as all-hadronic[15][16] ($VV \to q\bar{q}q\bar{q}$), semi-leptonic[10] ($VV \to l\bar{l}q\bar{q}$, $VV \to l\nu q\bar{q}$, $VV \to \nu\bar{\nu}q\bar{q}$), and all-leptonic[17] ($VV \to l\nu l\nu$, $VV \to l\bar{l}l\bar{l}$). Although conclusions from these different channels are statistically independent, it is important to remember that they often share the same background and signal simulations, and estimations related to detectors and integrated luminosity. This introduces correlations in the systematics of these channels that need to be treated as such in the statistical analyses[1].

These decay channels all share the single top and $t\bar{t}$ production backgrounds and the irreducible non-resonant diboson background[18]. Additionally, the decay channels with quarks have multijet and W/Z+jets backgrounds. Another significant background for the all-hadronic channel is a single quark or gluon jet being mistakenly identified as a V-jet. For semi-leptonic final states, high missing E^T and azimuthal angular separations between missing momentum and energy requirements are set for event selection to reduce the large

multi-jet background expected at low missing transverse energy E_T. As one might expect, it is difficult to reconstruct events with two neutrinos so this is rarely done. In general, for any decay channel with at least one missing neutrino, the requirement for event selection is very high missing E_T.

3.4 Statistical procedure

Once objects have been reconstructed and identified, we need to determine whether they correspond to an excess. To do this, control and signal regions are delineated based on selection criteria for objects. A maximum likelihood function $L(\mu, \vec{\theta})$ is defined, where μ is the signal strength and $\vec{\theta}$ is a set of nuisance parameters that can account for both the signal and the background properties. This function is calculated for bins of the discriminating variable in the control region. The discriminant is always chosen to be the reconstructed mass of the final decay state; apart from final states with more than one neutrino where transverse mass is used instead[10]. The mass ranges considered vary from study to study but are usually between 500 to 4000 GeV. A profile-likelihood-ratio test statistic is then used to calculate the p-values that signify the compatibility of the data with the background-only hypothesis[9]. This test is also used to determine the compatibility with the background plus signal hypothesis.

Both background and signal estimations are obtained from a combination of theory predictions and Monte Carlo simulations. Exceptions to this are multi-jet backgrounds that are very complex to simulate accurately so data from control regions is used to estimate them. Similarly, control region data is used to normalize W/Z + jets background contributions as their theoretical cross sections are usually less accurate in this region of the phase space[10]. All generated events are post-processed with detector simulation programs and the same trigger and reconstruction algorithms used on the actual data are applied to ensure correspondence of data and simulations.

As for systematic uncertainties, the major sources of experimental uncertainties are in relation to jet energy scales, the identification of particles, and the calculation of missing E_T. Theoretical uncertainties arise from the choice of parton distribution functions, event generators, and other simulations and models used. Systematics are incorporated into the likelihood functions through nuisance parameters.

4 Results and limits

We now look at the results that have been produced and the limits that have been set with these methods.

4.1 Run 1 results

The main anomaly in Run 1 was an excess at an invariant mass of 1.9 TeV found by an ATLAS search in the all-hadronic channel of $W' \to WZ$[19]. From the right plot in figure 3 we can see that this had a local significance of 3.4 σ, which corresponded to a global significance of 2.5 σ and an inferred production cross-section of 10 fb[18].

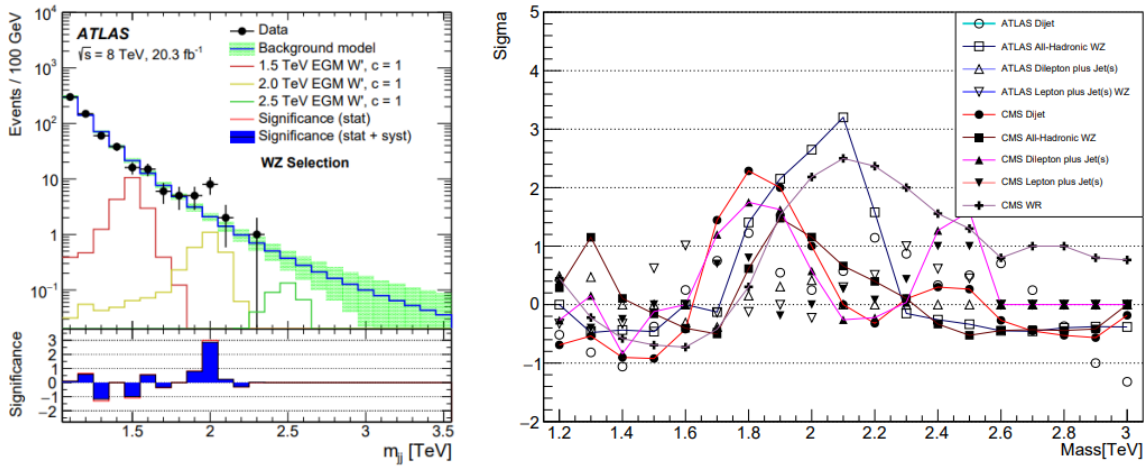

Figure 3: On the left, the background only fit to the dijet mass of a WZ decay with associated standard deviations[19]. On the right, the excesses in standard deviations compatible with a charged resonance from a collection of ATLAS and CMS run 1 searches[2].

CMS searches found excesses in the all-hadronic[20] and in one of the semi-leptonic[21] channels at the same invariant mass, but the highest global significance found was 1.5 σ. Searches in the other semi-leptonic and the all-leptonic channels did not find any excesses despite models not disfavouring them. A collection of all CMS and ATLAS run 1 excesses compatible with a charged resonance (like W') with a local significance above 1.5 σ can be found in the left plot of figure 3.

With this disagreement between channels, there was a lot of hope that run 2 would bring clearer and stronger results. In fact, with the increase in center of mass energy from 8 to 13 TeV, it was predicted that the Drell-Yan production of this charged would have a 5-7 times higher rate[2], theoretically allowing for a lot more events to be observed.

4.2 Run 2 results

As run 2 data started being collected and results started to get published, it became increasingly clear that the excesses from run 1 were attributable to statistical fluctuations. In figure 4 we can see the same all-hadronic WZ (combined with WW) analysis repeated with run 2 data. With the larger amount of data available, the excess at an invariant mass of 1.9 TeV has a local significance of less than 2 σ. These results are then interpreted in the context of the specific benchmark models detailed in section 2.2 to obtain limits on the masses and production cross-sections of the theorized resonances. These limits are set separately for each model and within those, for each channel. A recap of the latest ATLAS limits can be found in figure 5.

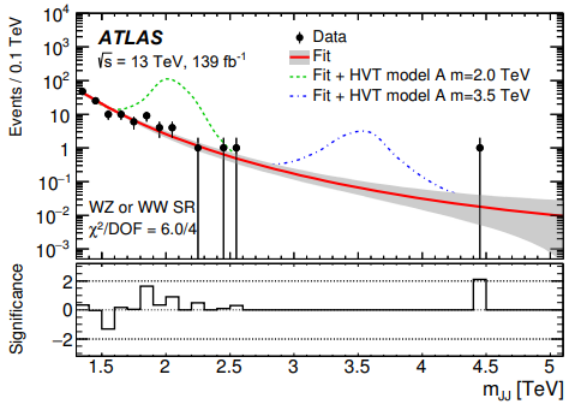

Figure 4: Background-only fit to the dijet mass distribution for combined $WW + WZ$ decays[16].

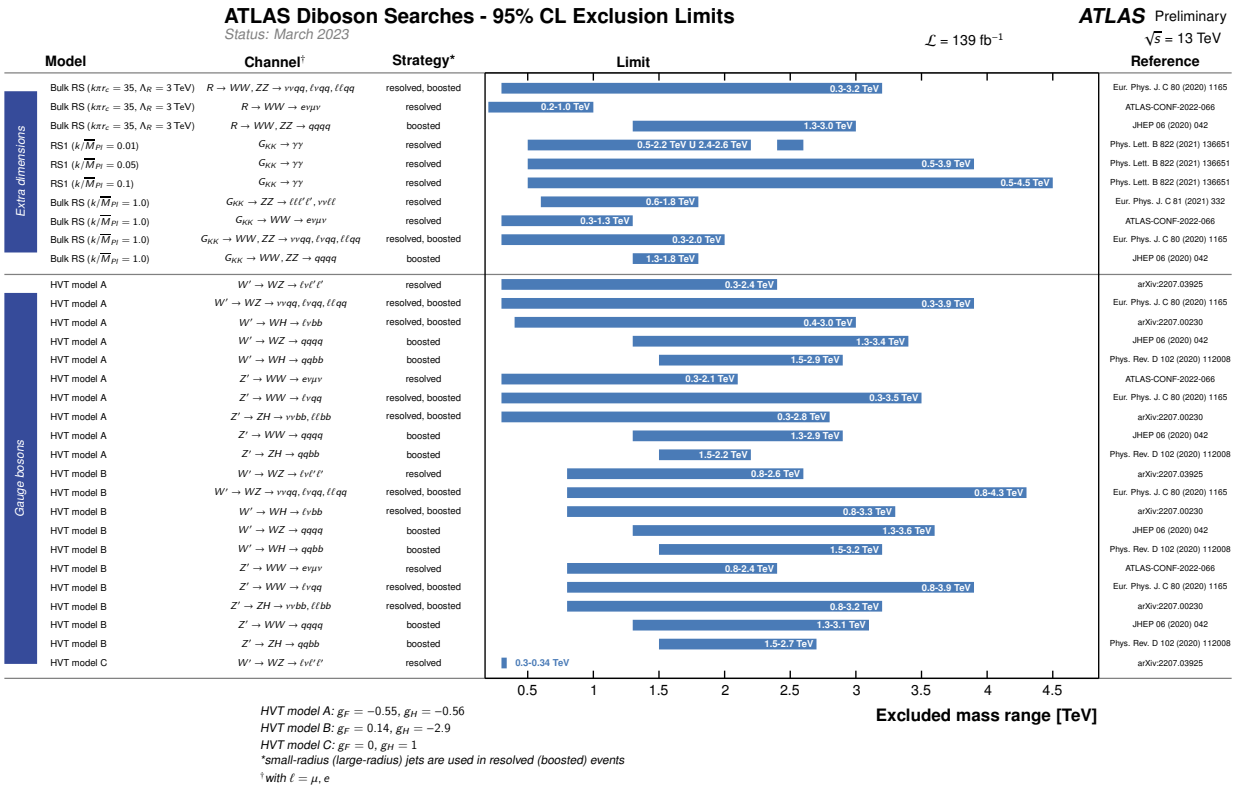

Figure 5: Summary of the March 2023 ATLAS mass limits of an RS radion and graviton and of an HVT W'/Z'[22].

4.3 Outlooks and considerations

Despite the fact that these searches have not found a diboson resonance, they have not been fruitless, Indeed, like many BSM searches, they have led to advancements in techniques and models used and have produced further evidence of the validity of the Standard Model.

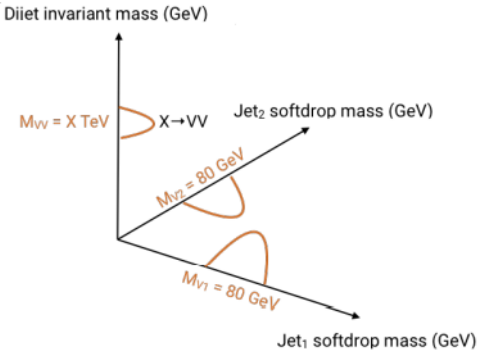

Figure 6: Comparison between the signal peak in one dimension and in the jet pair mass hyperplane[15].

One of the new techniques developed to improve the sensibility of these searches is a multi-dimensional fit method where instead of only inspecting pairs of jets with a mass comparable with the W/Z mass, this approach considers the entire hyperplane formed by the mass of each jet and their dijet invariant mass as a potential location for a resonance to emerge[15]. With this method, for an excess to be classified as a signal, it must peak in all three dimensions, as shown in figure 6. Consequently, it becomes less likely for background fluctuation to be mistakenly identified as signal events. This approach thus probes a wide range of masses at once, with an increased chance of finding a resonance not predicted by the current models and with a reduced risk of misidentification.

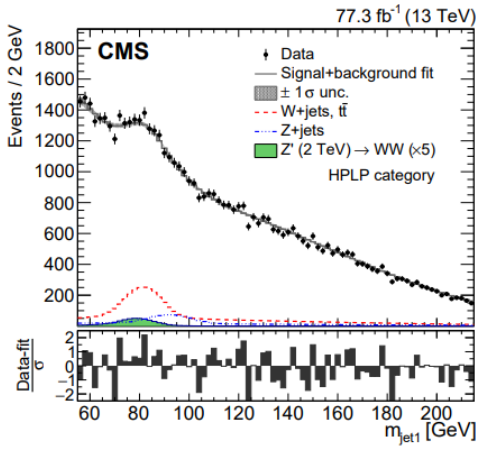

Figure 7: Signal + background fit and data distributions for the mass of one of the two jets. W+jets and Z+jets background have well-defined peaks in blue and red[15].

Thanks to advancements in techniques like this one, during run 2 the CMS experiment measured W/Z + jets SM backgrounds for the first time in a diboson analysis[15]. The peaks can be seen in figure 7. Their extracted cross-sections matched the SM predictions. This measurement not only further validates the SM but also enhances the sensitivity of the analysis by reducing uncertainties associated with the signal yield.

While we keep on searching for resonances at higher energies and set more stringent limits, it is important to remember that the data we currently have still has the potential not only to find diboson resonances with constantly improving techniques but also to further test and verify the Standard Model as we probe phase-space that we would not have otherwise.

References

[1] ATLAS Collaboration. Combination of searches for ww, wz, and zz resonances in pp collisions at $\sqrt{s} = 8$ tev with the atlas detector. *Physics Letters B*, 755, April 2016. ISSN 03702693. doi: 10.1016/j.physletb.2016.02.015. arXiv:1512.05099 [hep-ex].

[2] Brehmer et al. The diboson excess: Experimental situation and classification of explanations; a les houches pre-proceeding. (arXiv:1512.04357), December 2015. URL `http://arxiv.org/abs/1512.04357`. arXiv:1512.04357 [hep-ph].

[3] Leonard Susskind. Dynamics of spontaneous symmetry breaking in the weinberg-salam theory. *Phys. Rev. D*, 20:2619–2625, Nov 1979. doi: 10.1103/PhysRevD.20.2619. URL `https://link.aps.org/doi/10.1103/PhysRevD.20.2619`.

[4] Kenneth Lane. An introduction to technicolor. In *The Building Blocks of Creation*. World Scientific, October 1994. doi: 10.1142/9789814503785_0010. URL `http://dx.doi.org/10.1142/9789814503785_0010`.

[5] Koichi Yamawaki. *Old Wine in a New Bottle: Technidilaton as the 125 GeV Higg*, page 274–293. doi: 10.1142/9789813231467_0037. URL `https://www.worldscientific.com/doi/abs/10.1142/9789813231467_0037`.

[6] Hidenori S. Fukano, Masafumi Kurachi, Shinya Matsuzaki, Koji Terashi, and Koichi Yamawaki. 2 tev walking technirho at lhc? *Physics Letters B*, 750, November 2015. ISSN 0370-2693. doi: 10.1016/j.physletb.2015.09.023. URL `http://dx.doi.org/10.1016/j.physletb.2015.09.023`.

[7] Chuan-Hung Chen and Takaaki Nomura. 2 tev higgs boson and diboson excess at the lhc. *Physics Letters B*, 749, October 2015. ISSN 0370-2693. doi: 10.1016/j.physletb.2015.08.028.

[8] Walter D. Goldberger and Mark B. Wise. Modulus stabilization with bulk fields. *Physical Review Letters*, 83(24), December 1999. ISSN 1079-7114. doi: 10.1103/physrevlett.83.4922. URL `http://dx.doi.org/10.1103/PhysRevLett.83.4922`.

[9] ATLAS Collaboration. Searches for heavy diboson resonances in pp collisions at $\sqrt{s} = 13$ tev with the atlas detector. *Journal of High Energy Physics*, 2016(9):173, September 2016. ISSN 1029-8479. doi: 10.1007/JHEP09(2016)173. arXiv:1606.04833 [hep-ex].

[10] ATLAS Collaboration. Search for heavy diboson resonances in semileptonic final states in pp collisions at $\sqrt{s} = 13$ tev with the atlas detector. April 2021. doi: 10.1140/epjc/s10052-020-08554-y. URL `http://arxiv.org/abs/2004.14636`. arXiv:2004.14636 [hep-ex].

[11] Duccio Pappadopulo, Andrea Thamm, Riccardo Torre, and Andrea Wulzer. Heavy vector triplets: bridging theory and data. *Journal of High Energy Physics*, 2014(9):60, September 2014. ISSN 1029-8479. doi: 10.1007/JHEP09(2014)060.

[12] Tommaso Dorigo. Hadron collider searches for diboson resonances. *Progress in Particle and Nuclear Physics*, 100, May 2018. ISSN 01466410. doi: 10.1016/j.ppnp.2018.01.009. arXiv:1802.00354 [hep-ex, physics:hep-ph].

[13] Daniele Bertolini, Philip Harris, Matthew Low, and Nhan Tran. Pileup per particle identification. *Journal of High Energy Physics*, 2014(10), October 2014. ISSN 1029-8479. doi: 10.1007/jhep10(2014)059. URL http://dx.doi.org/10.1007/JHEP10(2014)059.

[14] Huang Huang. Searches for diboson resonances at cms. (arXiv:1710.05230), October 2017. doi: 10.48550/arXiv.1710.05230. URL http://arxiv.org/abs/1710.05230. arXiv:1710.05230 [hep-ex].

[15] Thea Aarrestad. Searching for diboson resonances in the boosted all-hadronic final state at s = 13 tev with cms. *Modern Physics Letters A*, 35(32):2030014, July 2020. ISSN 1793-6632. doi: 10.1142/s0217732320300141. URL http://dx.doi.org/10.1142/S0217732320300141.

[16] ATLAS Collaboration. Search for diboson resonances in hadronic final states in 139 fb^{-1} of pp collisions at $\sqrt{s} = 13$ tev with the atlas detector. *Journal of High Energy Physics*, 2019(9):91, September 2019. ISSN 1029-8479. doi: 10.1007/JHEP09(2019)091. arXiv:1906.08589 [hep-ex].

[17] ATLAS Collaboration. Search for heavy resonances decaying into a pair of z bosons in the $\ell^+\ell^-\ell'^+\ell'^-$ and $\ell^+\ell^-\nu\bar{\nu}$ final states using 139 fb^{-1} of proton-proton collisions at $\sqrt{s} = 13$ tev with the atlas detector. February 2022. doi: 10.1140/epjc/s10052-021-09013-y. URL http://arxiv.org/abs/2009.14791. arXiv:2009.14791 [hep-ex].

[18] Flavia A. Dias and (On behalf ofthe CMS Collaboration). Search for exotic resonances in diboson final states with the cms detector at the lhc. *Journal of Physics: Conference Series*, 455(1):012029, August 2013. ISSN 1742-6596. doi: 10.1088/1742-6596/455/1/012029.

[19] ATLAS Collaboration. Search for high-mass diboson resonances with boson-tagged jets in proton-proton collisions at $\sqrt{s} = 8$ tev with the atlas detector. *Journal of High Energy Physics*, 2015(12):1–39, December 2015. ISSN 1029-8479. doi: 10.1007/JHEP12(2015)055. arXiv:1506.00962 [hep-ex].

[20] CMS Collaboration. Search for massive resonances in dijet systems containing jets tagged as w or z boson decays in pp collisions at sqrt(s) = 8 tev. *Journal of High Energy Physics*, 2014(8):173, August 2014. ISSN 1029-8479. doi: 10.1007/JHEP08(2014)173. arXiv:1405.1994 [hep-ex].

[21] CMS Collaboration. Search for massive resonances decaying into pairs of boosted bosons in semi-leptonic final states at sqrt(s) = 8 tev. *Journal of High Energy Physics*, 2014(8):174, August 2014. ISSN 1029-8479. doi: 10.1007/JHEP08(2014)174. arXiv:1405.3447 [hep-ex].

[22] URL https://atlas.web.cern.ch/Atlas/GROUPS/PHYSICS/PUBNOTES/ATL-PHYS-PUB-2023-007/.